HHS Public Access

Author manuscript

Methods Cell Biol. Author manuscript; available in PMC 2017 February 10.

Published in final edited form as:

Methods Cell Biol. 2015 ; 127: 445–456. doi:10.1016/bs.mcb.2015.01.001.

Total Internal Reflection Fluorescence Microscopy of Intraflagellar Transport in *Tetrahymena thermophila*

Yu-Yang Jiang, **Karl Lechtreck**, and **Jacek Gaertig**

Department of Cellular Biology, University of Georgia, Athens, GA 30602

Abstract

Live imaging has become a powerful tool in studies of ciliary proteins. *Tetrahymena thermophila* is an established ciliated model with well developed genetic and biochemical approaches, but its large size, complex shape and the large number of short and overlapping cilia, have made live imaging of ciliary proteins challenging. Here we describe a method that combines paralysis of cilia by nickel ions and total internal reflection microscopy for live imaging of fluorescent proteins inside cilia of *Tetrahymena*. Using this method, we quantitatively documented the intraflagellar transport in *Tetrahymena*.

Keywords

IFT; dynein; kinesin; cilia; ciliate

I. Introduction

Many features make *Tetrahymena thermophila* an excellent model for studies of cilia, including the large number of cilia per cell, rapid growth in axenic media, and high maximal cell density (1×10^6 cells/ml), (reviewed in Gaertig, Wloga, Vasudevan, Guha, and Dentler (2013)). Each *Tetrahymena* cell possesses between 500–1000 locomotory and oral cilia that can be excised from the cell body by artificial deciliation, which triggers rapid regeneration of a new set of cilia (Calzone & Gorovsky, 1982; Rosenbaum & Carlson, 1969). The *Tetrahymena* population can be synchronized in the cell cycle either by starvation (Mowat, Pearlman, & Engberg, 1974) or by size selection using centrifugation/elutriation (Marsh, Cole, Stuart, Campbell, & Romero, 2000). Classical genetics (including ability to make whole genome homozygotes) can be combined with gene targeting by homologous DNA recombination (reviewed by Orias (2012)). Conditional gene overexpression based on heavy metal-inducible promoters can be used to produce and purify proteins or to create hypermorphic phenotypes (Shang, Song, et al., 2002). Gene products can be localized with precision by fusion with an epitope tag at the native loci (reviewed in Gaertig et al. (2013)). While detection of gene products of interest can be done with ease in fixed cells using fluorescence or electron microscopy, live imaging of fluorescence-tagged proteins has been used only sparingly (reviewed in Winey, Stemm-Wolf, Giddings, and Pearson (2012)).

Imaging ciliary proteins *in vivo* has been technically challenging in *Tetrahymena*. In particular, studies of the intraflagellar transport (IFT) have been limited by the lack of an imaging solution. IFT is a bidirectional motility that occurs inside cilia and is required for

assembly and maintenance of cilia. During IFT, motor proteins, kinesin-2 and IFT dynein (DH1B), move protein complexes, IFT trains, along the side of outer doublet microtubules; the IFT trains carry ciliary precursors as cargo (reviewed in (Pedersen & Rosenbaum, 2008; Scholey, 2003)). IFT was discovered in cilia of *Chlamydomonas reinhardtii* by video-enhanced differential interference microscopy (Kozminski, Johnson, Forscher, & Rosenbaum, 1993). More recently, the total internal reflection fluorescence (TIRF) microscopy (TIRFM) was applied to imaging of fluorescence-tagged IFT proteins in cilia of *Chlamydomonas* (Engel, Lechtreck, et al., 2009; Lechtreck, 2013). TIRFM involves selective illumination of objects located close to the coverglass surface (30–300 nm). TIRFM is highly suitable for imaging of cilia (~200 nm diameter), that in *Chlamydomonas* naturally tend to adhere to a smooth coverglass surface. (Collingridge, Brownlee, & Wheeler, 2013; Engel, Lechtreck, et al., 2009). Dual color TIRFM can be used to simultaneously detect proteins of the IFT trains and their cargoes (Lechtreck et al., 2009; Wren et al., 2013). Image processing software and analytical algorithms are used to produce kymographs of moving IFT components and to quantify their velocities, event frequencies and even the sizes of IFT trains (Ludington, Wemmer, Lechtreck, Witman, & Marshall, 2013).

Not limited to imaging of IFT, TIRFM is highly suitable for detection of non-abundant ciliary proteins, and tracking of ciliary protein dynamics in real time. TIRFM has brought new information about the mechanisms that govern cilia assembly, disassembly, length regulation and cilia-based signaling (Avasthi & Marshall, 2012; Engel, Ludington, & Marshall, 2009; Lechtreck et al., 2009; Ludington et al., 2013; Pan & Snell, 2014; Wren et al., 2013). Here we describe an approach that allows the application of TIRFM to study IFT in *Tetrahymena*. Combined with the existing biochemical, genetic and traditional microscopy capabilities, TIRFM-based live imaging greatly increases the value of the *Tetrahymena* model for studies of cilia.

II. TIRF microscope configuration and data analysis in application to IFT in *Tetrahymena*

The configuration of the TIRF microscope is the same as recently described for *Chlamydomonas* (Lechtreck, 2013). In brief, we used a TIRF system house-built around a Nikon Eclips Ti-U microscope. The microscope is equipped with a GFP/mCherry TIRF filter cube, a 60× NA 1.49 TIRF objective and an Andor iXON X3 DU897 EMCCD camera (with a C mount and a 2.5 × lens). The GFP is excited using a 488-nm diode laser, 40 mW (Spectraphysics) with two density filter wheels (Newport) to adjust the illumination intensity. The images and videos are digitally recorded with the Nikon Elements emission software module.

The analysis of imaging data is also adopted from Lechtreck (2013). NIH ImageJ (Rasband, 1997–2014) was used to generate kymographs and measure IFT particle velocities. In brief, videos of 30 sec were recorded at a frame rate of 15 fps. Some of the videos are not suitable because the imaged cells are not sufficiently immobilized (see III.B.). A high quality video typically covers a few dozens of cilia with detectable IFT in one cell. Only a handful of

these cilia are selected for generating kymographs of IFT particles. The individual cilia that are suitable for the production of kymographs fulfill the following criteria: 1) remain in focus along the entire length, 2) are relatively straight and remain immobile, 3) do not overlap with other cilia and 4) their base to tip orientation can be determined. Using ImageJ, a straight line is manually drawn to highlight the selected cilium, from its base to the tip. Then a kymograph is generated with the "Multiple Kymograph" function of the Kymograph plugin (Rietdorf & Seitz, 2004) of ImageJ. After rotating the kymograph 90 degree counterclockwise, the time lapses from left to right and the bottom of the image indicate the base of the cilium. A diagonal trajectory shown in the kymograph represent an actively moving IFT particle. An anterograde IFT will result in a trajectory from left-bottom to right-top, and a retrograde IFT will produce a trajectory from the left-top to the right-bottom. The velocity is measured as the distance divided by the time period of an IFT movement.

III. Using a TIRF microscope to image *Tetrahymena* cilia

Tetrahymena cells are challenging for live imaging of cilia. The cells move rapidly and do not adhere to glass. The *Tetrahymena* cell has a relatively large diameter (20–60 μm) compared to the length of the cilia (about 6 μm), and the locomotory cilia are located inside cortical grooves (reviewed in Wloga and Frankel (2012)). Despite the absence of chloroplasts, there is noticeable autofluorescence in the cell body that interferes with imaging even at a steep TIRF illuminating angle. When the cells are trapped under the coverglass, the cilia overlap and bundle. Consequently, the positions of the ciliary tips and the bases are difficult or impossible to determine, preventing the orientation of IFT tracks. Our approach to reduce the impact of some of these obstacles was to combine trapping of cells in a limited volume of medium with immobilization of cilia using nickel ions (see III.B.).

A. GFP-Dyf1 is a suitable IFT marker in *Tetrahymena*

Using TIRFM, we tested several GFP-tagged IFT proteins as markers for imaging IFT, including Kin1p, a motor subunit of kinesin-2, the anterograde IFT motor (Brown, Marsala, Kosoy, & Gaertig, 1999), and components of the IFT complex B: Ift52p (Brown, Fine, Pandiyan, Thazhath, & Gaertig, 2003) and Dyf1p (Dave, Wloga, Sharma, & Gaertig, 2009). In each case, the GFP fusion was expressed in its own gene knockout background and rescued the loss of cilia phenotype, indicating its functionality. The GFP-Kin1p was expressed under its own promoter and in its own locus, while the GFP-Ift52p and the GFP-Dyf1p were expressed under the cadmium-inducible *MTT1* promoter (Shang, Li, & Gorovsky, 2002) in the non-essential *BTU1* locus (these cells were maintained without cadmium induction as the non-induced *MTT1* promoter has a basal level of expression that is sufficient for rescue of the respective null phenotype). GFP-Dyfp1 was found to be a superior IFT marker that revealed IFT tracks with the highest signal intensity and few stationary particles (supplemental videos 1 and 2).

B Immobilization of *Tetrahymena* cilia to observe IFT

Simply pressing the *Tetrahymena* cells with a coverglass does not immobilize most cilia sufficiently well. Occasionally, a cilium is sufficiently immobile for imaging but this is rare.

Most cilia continue to beat and at some point bundle (Fig. 1A). Among cilia that do not bundle, most do not lay straight (Fig. 1B). Neither bundled nor bent cilia are suitable for quantification of IFT events.

We tried several methods to immobilize *Tetrahymena* cells prior to TIRFM observations. Coating coverglasses with poly-L-lysine did not increase the adhesion and immobilization of cells. Embedding cells in 2–5% low melting temperature point agarose resulted in encapsulation of cells, which maintain vigorously beating cilia (the agar failed to solidify in a narrow zone around beating cilia). We found that the most practical immobilization method is simply placing cells in a small volume of media, which results in a pressure from the coverglass that flattens the cells and presses the cilia against the glass, and allows for a 15–25 min observation, before the cells burst. Under these conditions, however, most cilia continue to twitch and the number of cilia suitable for imaging is very low.

To further reduce the motility of cilia, in one attempt we labeled the surface of cells with NHS-LC-LC-biotin, and mounted onto a coverglass coated with streptavidin. The attachment of biotinylated cilia to the streptavidin-coated coverglass was noticeable, yet too weak to hold the cilia sufficiently stable for a 30 sec recording, as the cilia continued to twitch. We had similar negative experiences with the use of coverglasses coated with lectins, (concanavalin A, peanut agglutinin). We then used Ni^{2+} ions, an established axonemal dynein inhibitor, to inhibit ciliary beating (Larsen & Satir, 1991). We found that in the presence of 2–3 μM $NiCl_2$, the cells stop moving within 3 min and most cilia remain immobile when pressed against the glass. In the Ni^{2+} observation medium (see section III.C.), the cells burst within 10–15 min post mounting. Most cells treated with Ni^{2+} are suitable for recording. For each microscope slide, we were able to record about ten 30 sec videos, each covering a large number of cilia on one cell (supplemental videos 1 and 2). Under these conditions, the anterograde IFT is slower, more frequent and uniform in size, as compared to the retrograde IFT (Fig. 2). We noticed a significant variation in the frequencies of both the anterograde and retrograde IFT events between cilia on one cell and between different cells, which is likely a result of differential pressure against the glass (see section IV).

C. Experimental Protocol

1. Preparation of *Tetrahymena* cells:
    1. Grow cells in SPP medium to 1–3 × 105 cells/ml.
    2. Pellet 0.5–1 ml of cell culture by centrifugation at 1700 × g for 1 min.
    3. Wash the pellet once with 10 mM Tris-HCl, pH 7.5 (Tris buffer).

       This step is optional but highly recommended as it reduces the background of fluorescent debris from the medium.
    4. Suspend the cells in 100–300 μl of Tris buffer.
2. Preparation of a slide specimen for TIRF imaging:

1. Mix 1 μl of 20 μM NiCl2 and 10 μl of washed cells (final concentration of $NiCl_2$ is 2 μM) at the center of a 22 × 22 mm^2 No. 1.5 coverglass (VWR #48366-227). If the cells are imaged in the SPP medium (containing 0.003% w/v EDTA-Fe-Na) a higher concentration of $NiCl_2$ may be needed.
2. Use a glass slide to gently touch the droplet, and pick the coverglass up, forming an upside down assembled slide.
3. Mount the assembled slide onto the microscope stage with the coverglass facing down and hanging over the objective. Be cautious as flipping, shaking or resting the assembly will cause the coverglass to glide and this will crush the cells or rip off the cilia.

3. Recording images and videos of cilia and IFT:
   1. Using bright-field illumination, find the correct focal position.
   2. As the cells slow down within the first few min, the larger cells flatten first and the cilia at the mid-section of their cell bodies become “squeezed” onto the coverglass. Such cilia are optimal for imaging IFT as they are flat, uniformly close to glass and often aligned in one direction.
   3. Perform TIRF imaging at a sufficiently steep angle to avoid autofluorescence of the cell bodies.
   4. Under the above conditions, most slides last for 10–15 min. As the cells round up, IFT events become slower and less frequent and soon the cells burst. We avoid recording videos of IFT after the first 10 min since the slide assembles.

D. Effect of Ni^{2+} on the velocities of IFT

We were concerned about the potential side effect of Ni^{2+} on the retrograde IFT driven by the cytoplasmic dynein that contains the heavy chain DH1B (Pazour, Dickert, & Witman, 1999; Signor et al., 1999). However, unlike another dynein inhibitor, vanadate, that decreases the ATPase activity of both the axonemal outer and inner dynein arm (ODA and IDA) (Gibbons et al., 1978; Vale & Toyoshima, 1988) and the cytoplasmic dynein heavy chains (Cande & Wolniak, 1978; Kobayashi, Martensen, Nath, & Flavin, 1978), Ni^{2+} abolishes IDA, but has only a minor effect on the ODA ATPase activity (Larsen & Satir, 1991), suggesting a degree of selectivity toward dynein subtypes. The retrograde IFT dynein heavy chain, DH1B, belongs to the cytoplasmic dynein subgroup of the dynein superfamily, that is evolutionarily distant from both IDA and ODA axonemal dyneins (Wickstead & Gull, 2007; Wilkes, Watson, Mitchell, & Asai, 2008). Nevertheless, we could not exclude a possibility that Ni^{2+} has a side effect on the IFT dynein heavy chain and consequently on the retrograde IFT in *Tetrahymena*.

We compared the anterograde and retrograde IFT velocities in the Ni^{2+} treated and untreated cells (while fewer cilia were suitable for imaging without Ni^{2+} immobilization, we were able

to gather enough of data by examining a larger number of untreated cells). Using GFP-Dyf1p as a marker, the velocities of IFT particles were measured as is described in section II. To our surprise, the mean velocities of the anterograde and retrograde IFT of Ni^{2+} treated cilia were significantly higher than those from the untreated cilia (Fig. 3A, B). Both the anterograde and retrograde IFT velocities were increased by about 25%, suggesting the effect of Ni^{2+} is grounded in the methodology and does not reflect a real stimulatory effect of Ni^{2+} on the IFT motors.

We noticed that the IFT velocities histograms of the Ni^{2+}-treated cilia fit the normal distribution curves, while those of the untreated cilia lean towards the lower values (Fig. 3A′, B′). Using an approach similar to ours, Brooks and Wallingford (2012) measured the velocities of the anterograde and retrograde IFT in *Xenopus* multiciliated cells, in cilia that were pressed against the coverglass by the gravity of the embryos. Their reported histograms of IFT velocities appear to fit the normal distribution (Figure 2 in Brooks and Wallingford (2012)), which are in agreement with our measurements from the Ni^{2+}-treated cilia. The simplest interpretation of the effect of Ni^{2+} in our experiments is that the slower IFT velocities of untreated cilia are an artifact caused by the inability to distinguish between cilia or their segments that lay flat on the cover glass or slightly bend away from the glass. When using the Kymograph ImageJ plugin to analyze IFT velocity, it is crucial that the straight line is fitted to a straight cilium. If the straight line is fitted to a slightly curved cilium and used to calculate the velocity of an IFT movement, the measured velocity is the true velocity times the cosine of the curving angle. Curved cilia are clearly more frequent in untreated specimens (Fig. 1). Ni^{2+} rapidly impairs cilia motility and reduces cilia curving and bundling. In addition, Ni^{2+}-treated cilia are often aligned in one direction (Fig. 1C). This may be caused by a small drift of the cell body after cilia paralysis. In summary, Ni^{2+} does not appear to affect the IFT DH1B dynein and its paralyzing effect on cilia greatly facilitates the scale and quality of IFT imaging.

IV. Limitations

Our method is the first step towards routine employment of live imaging tools such as TIRFM to study of ciliary proteins in *Tetrahymena*. To our knowledge, we are first to report the velocities of IFT for *Tetrahymena*. There are certain limitations of our approach. In particular, there is major variability in the frequency and intensity of IFT particles between different cells on the same slide and even among individual cilia within the same cell. This makes the determination of IFT event frequency and estimation of the IFT particle size distribution challenging. In contrast to the *Chlamydomonas* TIRF approach that relies on the natural adhesion of flagella to glass, in our method, the cilia of *Tetrahymena* are pressed against but do not adhere to glass. The closeness of the imaged cilia to the coverglass varies between different cells depending on the degree of their flattening, which in turn depends on the cell size (cell cycle stage), the side on which the cell lands on glass (ventral, dorsal, lateral), and the local differences in the medium layer height across the coverglass. Within the same cell, different cilia experience a different level of pressure against the glass depending on their position on the antero-posterior and circumferential axes, and whether they are immobilized between or along the cortical grooves. In TIRFM, the energy exciting the fluorescence decreases exponentially with the distance away from the coverglass. Thus, a

slight variation in the closeness of cilia to the coverglass can greatly affect the intensity of the ciliary signals.

Nevertheless, even with the current limitations, our approach can be used to determine the IFT velocities. In the future, dual color imaging should be feasible to simultaneously image cargoes and IFT trains. Multiple selectable markers (Chalker, 2012; Iwamoto, Mori, Hiraoka, & Haraguchi, 2014) will allow for incorporation of IFT markers into various gene knockout backgrounds, to enable functional studies on the mechanism of IFT.

Supplementary Material

Refer to Web version on PubMed Central for supplementary material.

Acknowledgments

We acknowledge the support of research in our laboratories by grants from the National Institutes of Health (GM0571173 to JG and GM110413 to KL).

References

Avasthi P, Marshall WF. Stages of ciliogenesis and regulation of ciliary length. Differentiation. 2012; 83(2):S30–42. DOI: 10.1016/j.diff.2011.11.015 [PubMed: 22178116]

Brooks ER, Wallingford JB. Control of vertebrate intraflagellar transport by the planar cell polarity effector Fuz. J Cell Biol. 2012; 198(1):37–45. DOI: 10.1083/jcb.201204072 [PubMed: 22778277]

Brown JM, Fine NA, Pandiyan G, Thazhath R, Gaertig J. Hypoxia regulates assembly of cilia in suppressors of *Tetrahymena* lacking an intraflagellar transport subunit gene. Mol Biol Cell. 2003; 14(8):3192–3207. DOI: 10.1091/mbc.E03-03-0166 [PubMed: 12925756]

Brown JM, Marsala C, Kosoy R, Gaertig J. Kinesin-II is preferentially targeted to assembling cilia and is required for ciliogenesis and normal cytokinesis in *Tetrahymena*. Mol Biol Cell. 1999; 10(10): 3081–3096. [PubMed: 10512852]

Calzone FJ, Gorovsky MA. Cilia regeneration in *Tetrahymena*. A simple reproducible method for producing large numbers of regenerating cells. Exp Cell Res. 1982; 140(2):471–476. [PubMed: 7117410]

Cande WZ, Wolniak SM. Chromosome movement in lysed mitotic cells is inhibited by vanadate. J Cell Biol. 1978; 79(2 Pt 1):573–580. [PubMed: 152767]

Chalker DL. Transformation and strain engineering of *Tetrahymena*. Methods Cell Biol. 2012; 109:327–345. DOI: 10.1016/B978-0-12-385967-9.00011-6 [PubMed: 22444150]

Collingridge P, Brownlee C, Wheeler GL. Compartmentalized calcium signaling in cilia regulates intraflagellar transport. Curr Biol. 2013; 23(22):2311–2318. DOI: 10.1016/j.cub.2013.09.059 [PubMed: 24210618]

Dave D, Wloga D, Sharma N, Gaertig J. DYF-1 Is required for assembly of the axoneme in *Tetrahymena thermophila*. Eukaryot Cell. 2009; 8(9):1397–1406. DOI: 10.1128/EC.00378-08 [PubMed: 19581442]

Engel BD, Lechtreck KF, Sakai T, Ikebe M, Witman GB, Marshall WF. Total internal reflection fluorescence (TIRF) microscopy of *Chlamydomonas* flagella. Methods Cell Biol. 2009; 93:157–177. DOI: 10.1016/S0091-679X(08)93009-0 [PubMed: 20409817]

Engel BD, Ludington WB, Marshall WF. Intraflagellar transport particle size scales inversely with flagellar length: revisiting the balance-point length control model. J Cell Biol. 2009; 187(1):81–89. DOI: 10.1083/jcb.200812084 [PubMed: 19805630]

Gaertig J, Wloga D, Vasudevan KK, Guha M, Dentler W. Discovery and functional evaluation of ciliary proteins in *Tetrahymena thermophila*. Methods Enzymol. 2013; 525:265–284. DOI: 10.1016/B978-0-12-397944-5.00013-4 [PubMed: 23522474]

Gibbons IR, Cosson MP, Evans JA, Gibbons BH, Houck B, Martinson KH, Tang WJ. Potent inhibition of dynein adenosinetriphosphatase and of the motility of cilia and sperm flagella by vanadate. Proc Natl Acad Sci U S A. 1978; 75(5):2220–2224. [PubMed: 149986]

Iwamoto M, Mori C, Hiraoka Y, Haraguchi T. Puromycin resistance gene as an effective selection marker for ciliate *Tetrahymena*. Gene. 2014; 534(2):249–255. DOI: 10.1016/j.gene.2013.10.049 [PubMed: 24185080]

Kobayashi T, Martensen T, Nath J, Flavin M. Inhibition of dynein ATPase by vanadate, and its possible use as a probe for the role of dynein in cytoplasmic motility. Biochem Biophys Res Commun. 1978; 81(4):1313–1318. [PubMed: 149544]

Kozminski KG, Johnson KA, Forscher P, Rosenbaum JL. A motility in the eukaryotic flagellum unrelated to flagellar beating. Proc Natl Acad Sci U S A. 1993; 90(12):5519–5523. [PubMed: 8516294]

Larsen J, Satir P. Analysis of Ni(2+)-induced arrest of Paramecium axonemes. J Cell Sci. 1991; 99(Pt 1):33–40. [PubMed: 1836792]

Lechtreck KF. In vivo imaging of IFT in *Chlamydomonas* flagella. Methods Enzymol. 2013; 524:265–284. DOI: 10.1016/B978-0-12-397945-2.00015-9 [PubMed: 23498745]

Lechtreck KF, Johnson EC, Sakai T, Cochran D, Ballif BA, Rush J, Witman GB. The *Chlamydomonas reinhardtii* BBSome is an IFT cargo required for export of specific signaling proteins from flagella. J Cell Biol. 2009; 187(7):1117–1132. DOI: 10.1083/jcb.200909183 [PubMed: 20038682]

Ludington WB, Wemmer KA, Lechtreck KF, Witman GB, Marshall WF. Avalanche-like behavior in ciliary import. Proc Natl Acad Sci U S A. 2013; doi: 10.1073/pnas.1217354110

Marsh TC, Cole ES, Stuart KR, Campbell C, Romero DP. RAD51 is required for propagation of the germinal nucleus in *Tetrahymena thermophila*. Genetics. 2000; 154(4):1587–1596. [PubMed: 10747055]

Mowat D, Pearlman RE, Engberg J. DNA synthesis following refeeding of starved *Tetrahymena pyriformis* GL: starved cells are arrested in G 1. Exp Cell Res. 1974; 84(1):282–286. [PubMed: 4206338]

Orias E. *Tetrahymena thermophila* genetics: concepts and applications. Methods Cell Biol. 2012; 109:301–325. DOI: 10.1016/B978-0-12-385967-9.00010-4 [PubMed: 22444149]

Pan J, Snell WJ. Organelle Size: A Cilium Length Signal Regulates IFT Cargo Loading. Curr Biol. 2014; 24(2):R75–78. DOI: 10.1016/j.cub.2013.11.043 [PubMed: 24456980]

Pazour GJ, Dickert BL, Witman GB. The DHC1b (DHC2) isoform of cytoplasmic dynein is required for flagellar assembly. J Cell Biol. 1999; 144(3):473–481. [PubMed: 9971742]

Pedersen LB, Rosenbaum JL. Intraflagellar transport (IFT) role in ciliary assembly, resorption and signalling. Curr Top Dev Biol. 2008; 85:23–61. DOI: 10.1016/S0070-2153(08)00802-8 [PubMed: 19147001]

Rasband, WS. ImageJ. U.S. National Institutes of Health; Bethesda, Maryland, USA: 1997–2014. http://imagej.nih.gov/ij/

Rietdorf J, Seitz A. ImageJ Kymograph. 2004

Rosenbaum JL, Carlson K. Cilia regeneration in *Tetrahymena* and its inhibition by colchicine. J Cell Biol. 1969; 40(2):415–425. [PubMed: 4882889]

Scholey JM. Intraflagellar transport. Annu Rev Cell Dev Biol. 2003; 19:423–443. DOI: 10.1146/annurev.cellbio.19.111401.091318 [PubMed: 14570576]

Shang Y, Li B, Gorovsky MA. *Tetrahymena thermophila* contains a conventional gamma-tubulin that is differentially required for the maintenance of different microtubule-organizing centers. J Cell Biol. 2002; 158(7):1195–1206. [PubMed: 12356864]

Shang Y, Song X, Bowen J, Corstanje R, Gao Y, Gaertig J, Gorovsky MA. A robust inducible-repressible promoter greatly facilitates gene knockouts, conditional expression, and overexpression of homologous and heterologous genes in *Tetrahymena thermophila*. Proc Natl Acad Sci U S A. 2002; 99(6):3734–3739. DOI: 10.1073/pnas.052016199 [PubMed: 11891286]

Signor D, Wedaman KP, Orozco JT, Dwyer ND, Bargmann CI, Rose LS, Scholey JM. Role of a class DHC1b dynein in retrograde transport of IFT motors and IFT raft particles along cilia, but not dendrites, in chemosensory neurons of living *Caenorhabditis elegans*. J Cell Biol. 1999; 147(3):519–530. [PubMed: 10545497]

Vale RD, Toyoshima YY. Rotation and translocation of microtubules in vitro induced by dyneins from *Tetrahymena* cilia. Cell. 1988; 52(3):459–469. [PubMed: 2964278]

Wickstead B, Gull K. Dyneins across eukaryotes: a comparative genomic analysis. Traffic. 2007; 8(12):1708–1721. DOI: 10.1111/j.1600-0854.2007.00646.x [PubMed: 17897317]

Wilkes DE, Watson HE, Mitchell DR, Asai DJ. Twenty-five dyneins in *Tetrahymena*: A re-examination of the multidynein hypothesis. Cell Motil Cytoskeleton. 2008; 65(4):342–351. DOI: 10.1002/cm.20264 [PubMed: 18300275]

Winey M, Stemm-Wolf AJ, Giddings TH Jr, Pearson CG. Cytological analysis of *Tetrahymena thermophila*. Methods Cell Biol. 2012; 109:357–378. DOI: 10.1016/B978-0-12-385967-9.00013-X [PubMed: 22444152]

Wloga D, Frankel J. From molecules to morphology: cellular organization of *Tetrahymena thermophila*. Methods Cell Biol. 2012; 109:83–140. DOI: 10.1016/B978-0-12-385967-9.00005-0 [PubMed: 22444144]

Wren KN, Craft JM, Tritschler D, Schauer A, Patel DK, Smith EF, Lechtreck KF. A differential cargo-loading model of ciliary length regulation by IFT. Curr Biol. 2013; 23(24):2463–2471. DOI: 10.1016/j.cub.2013.10.044 [PubMed: 24316207]

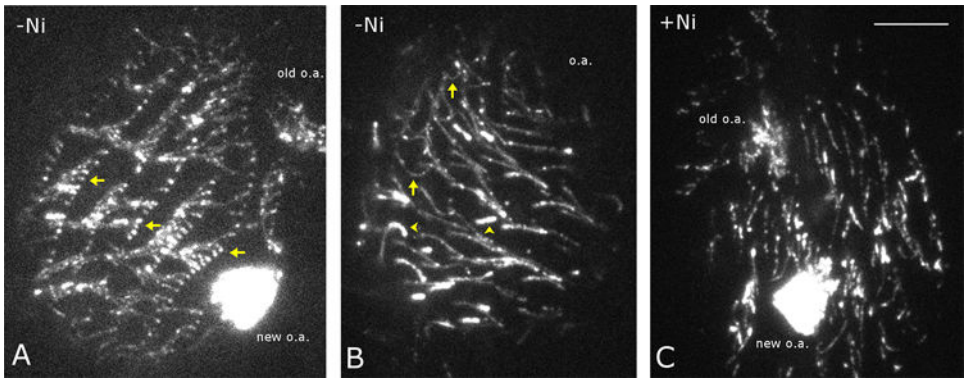

Figure 1. Inhibition of axonemal dynein with nickel ions improves the quality of live imaging of IFT in cilia of *Tetrahymena thermophila*

TIRF Images of *Tetrahymena* cells expressing GFP-Dyf1p. (A) A dividing cell that was not treated with Ni^{2+}. Note tangles of multiple cilia (arrows) that are not usable for measuring IFT. The old and new oral apparatuses are marked (o.a.). (B) A non-dividing cell that was not treated with Ni^{2+}. Many cilia are bent (arrows) and not suitable for measuring IFT. Note the (shorter) assembling cilia (arrowheads) have a higher GFP-Dyf1p signal intensity. (C) A cell that was treated with Ni^{2+}. Note that the cilia are relatively straight, and most cilia are not bundled. In addition, many cilia are aligned in the same direction facilitating the orientation of IFT events in the relation to the position of the basal bodies. Scale bar = 10 μm

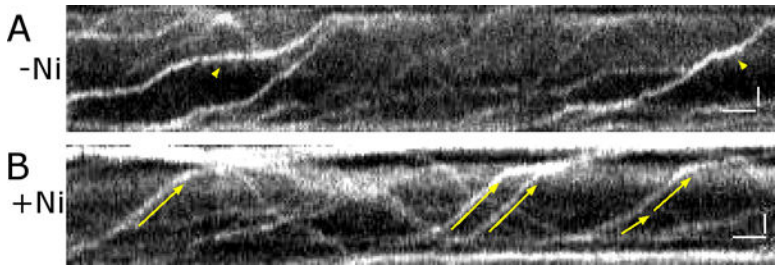

Figure 2. Bent or detached cilia can lead to artifacts when measuring the IFT velocity. Paralyzing cilia with Ni^{2+} reduces these artifacts

(A) A kymograph obtained for an untreated cilium that is likely to be partially detached from the coverglass surface at its mid-section. The arrowheads point at the segments of the tracks that appear fuzzier and where the apparent velocity rate is reduced. Such segments most likely represent a regions of the cilium that is detached from the coverglass surface. (B) A kymograph obtained for a Ni^{2+}-treated cilium. The IFT tracks (arrows) are sharp and consistent in the angle (velocity), indicating that the cilium is uniformly attached to the coverglass. Notice that the retrograde IFT particles are more varied in size as compared to the anterograde IFT particles. Time: left to right. The proximal end of the cilium is at the bottom. Scale bars = 1 second and 1 μm.

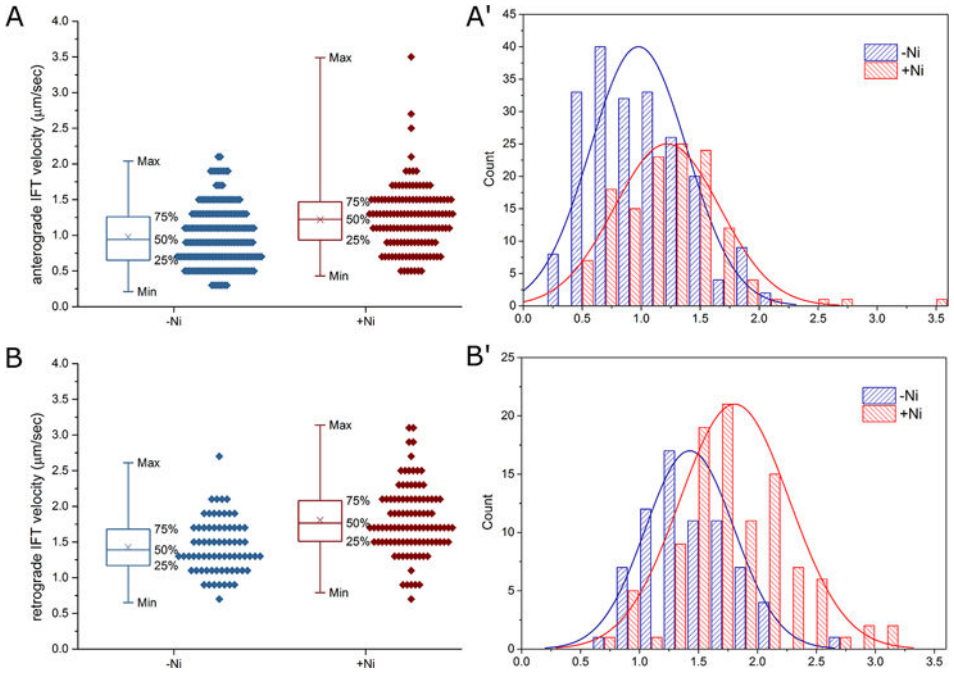

Figure 3. Inhibition of axonemal dynein with nickel ions does not have a side effect on IFT

The velocities of the anterograde (A) and retrograde (B) IFT, without (blue) or with Ni^{2+} treatment (red) are shown as data points along with their box and whisker plots. Crosses indicate the means. The measured untreated anterograde IFT velocity is 0.98 ± 0.01 µm/sec, n = 207. The measured Ni^{2+}-treated anterograde IFT velocity is 1.22 ± 0.02 µm/sec, n = 132. The difference is significant, $p < 1 \times 10^{-6}$. The measured untreated retrograde IFT velocity is 1.81 ± 0.02 µm/sec, n= 71. The measured Ni^{2+}-treated retrograde IFT velocity is 1.43 ± 0.02 µm/sec, n = 100. The difference is significant, $p < 1 \times 10^{-7}$. (A′, B′). The histograms of the same data sets as in A and B are compared with their normal distribution curves. The Ni^{2+}-treated anterograde and retrograde IFT velocities fit the normal distribution curves closely. The measured untreated anterograde and retrograde IFT velocities lean toward the lower values. In the absence of Ni^{2+} the measured velocities are likely to be underestimated due to curving and detachment of cilia (see Fig. 2).